Two-pion interferometry for partially coherent sources in relativistic heavy-ion collisions in a multiphase transport model

Shi-Yao Wang, Jun-Ting Ye, and Wei-Ning Zhang *
School of Physics, Dalian University of Technology, Dalian, Liaoning 116024, China

(Received 29 August 2023; accepted 5 January 2024; published 31 January 2024)

We perform two-pion Hanbury-Brown–Twiss (HBT) interferometry for the partially coherent pion-emitting sources in relativistic heavy-ion collisions using a multiphase transport (AMPT) model. A longitudinal coherent emission length, as well as a transverse coherent emission length, are introduced to the pion generation coordinates in calculating the HBT correlation functions of the partially coherent sources. We compare the model results with and without coherent emission conditions with experimental data in Au-Au collisions at center-of-mass energy $\sqrt{s_{NN}} = 200\,\text{GeV}$ and in Pb-Pb collisions at center-of-mass energy $\sqrt{s_{NN}} = 2.76\,\text{TeV}$, and find that the HBT results of the partially coherent sources are closer to the experimental data than those of chaotic sources.

DOI: 10.1103/PhysRevC.109.014912

I. INTRODUCTION

Two-pion Hanbury-Brown–Twiss (HBT) correlation is an important observable to detect the space-time structure of particle-emitting sources produced in relativistic heavy-ion collisions [1–6]. Because the two pions emitted coherently have no HBT correlation, this observable can also be used to study the source coherence [1–6]. Recent measurements of two-pion HBT correlations in Pb-Pb collisions at the Large Hadron Collider (LHC) [7–9] and measurements in Au-Au collisions at the Relativistic Heavy Ion Collider (RHIC) [10–13] showed that the two-pion correlation functions near zero relative momentum are substantially less than 2, corresponding to the magnitude for completely chaotic sources [1–6]. These observations and the suppression of the multipion correlation functions observed in Pb-Pb collisions at the LHC [7,14] indicate that the pion-emitting sources are perhaps partially coherent. However, there is no widely accepted explanation for these observations.

Because of the complexity of relativistic heavy-ion collision systems, the calculations for experimental observables based on models play an important role in understanding the system properties. A multiphase transport model (AMPT) has been extensively used in relativistic heavy-ion collisions [15–33]. In Ref. [34] the authors studied the two-pion HBT correlation functions for the partially coherent pion-emitting sources constructed with the AMPT model by introducing a coherent emission length L_C to the pion longitudinal freeze-out coordinates. It was assumed that the emission of the two pions with a longitudinal difference of freeze-out coordinates smaller than L_C is coherent, and otherwise it is completely chaotic [33]. They found that the intercepts of the two-pion correlation functions of the partially coherent sources with finite coherent emission lengths are less than those of the completely chaotic sources in Au-Au collisions at center-of-mass energy $\sqrt{s_{NN}} = 200\,\text{GeV}$, and in Pb-Pb collisions at center-of-mass energy $\sqrt{s_{NN}} = 2.76\,\text{TeV}$.

As a microscopic transport model, the AMPT model can provide the coordinates and momenta of the freeze-out particles at each time step in the source after they are generated. In this paper we introduce a transverse coherent emission length and a longitudinal coherent emission length, which are momentum dependent according to particle de Broglie wavelength, to identical pion generation coordinates to construct the partially coherent pion-emitting sources. We calculate the two-pion correlation functions for the partially coherent sources in the AMPT model and compare the model results with experimental data in Au-Au collisions at $\sqrt{s_{NN}} = 200\,\text{GeV}$ [12] and in Pb-Pb collisions at $\sqrt{s_{NN}} = 2.76\,\text{TeV}$ [9]. We find that the HBT results of partially coherent sources are closer to experimental data than those of chaotic sources. The results of coherent fraction for the partially coherent sources in Pb-Pb collisions are consistent with the values extracted from the experimental measurements of multipion HBT correlations [7,14].

The rest of this paper is organized as follows. Section II presents a brief introduction to the AMPT model and discusses the generation and freeze-out coordinates of identical pions generated by quark coalescence and by particle scattering and decay. Section III gives the two-pion correlation function calculations for the partially coherent and completely chaotic sources. Model HBT interferometry results in Au-Au collisions at $\sqrt{s_{NN}} = 200\,\text{GeV}$, and in Pb-Pb collisions at $\sqrt{s_{NN}} = 2.76\,\text{TeV}$, are presented and compared with experimental data at the RHIC and LHC. We summarize and discuss this work in Sec. IV.

*wnzhang@dlut.edu.cn

II. PION GENERATION AND FREEZE-OUT IN AMPT MODEL

The AMPT model is a hybrid composed of initialization, parton transport, hadronization, and hadron transport [17]. It has been successfully used to describe the observables in high-energy heavy-ion collisions at the RHIC and LHC [15–32]. The initialization of collisions in the AMPT model is performed using the HIJING model [35]. The parton and hadron transport are described by the ZPC (Zhangs parton cascade) model [36] and ART model [37], respectively. In this study we use the string melting version of the AMPT model in which partons are hadronized by the quark coalescence mechanism [15,17]. We take the model parameter μ of the parton screening mass to be 2.2814 fm^{-1} and the strong coupling constant α_s to be 0.47, corresponding to a parton-scattering cross section of 6 mb [17].

After hadronization, the generated hadrons may interact with other particles in the source and may be absorbed or remain until freeze-out. Some hadrons may also be generated by particle interactions in the source and hadron decays. With the AMPT model, we can trace back to the origin of a freeze-out particle, its generation coordinates, momentum, and parent. For instance, we can track back step-by-step for a recorded pion with freeze-out coordinate $\mathbf{r}_f$ to find its first appeared position $\mathbf{r}_g$, called generation coordinates, according to the recording files of the AMPT model. Figure 1 shows the average transverse and longitudinal freeze-out coordinates (dashed lines) and generation coordinates (solid lines) of identical pions versus the particle transverse momentum in Au-Au collisions at $\sqrt{s_{NN}} = 200$ GeV, where panels (a)–(c) are for all identical (negative) pions, the pions generated by quark coalescence, and the pions generated by particle scattering and hadron decays, respectively. In our calculations the cutoff time for a hadron cascade is taken to be 200 fm/c, as in previous HBT studies [17]. The impact parameter is taken to be 0–3 fm. For Au-Au collisions at $\sqrt{s_{NN}} = 200$ GeV, we take a rapidity cut, $|y| < 0.5$, as in experimental data analyses [12]. It can be seen that the average freeze-out coordinates are larger than the average generation coordinates. The average values for quark coalescence generation are the smallest, and the average values for the pions generated by particle scattering and decay are the largest. This is because pions generated by quark coalescence occur earlier on average than those generated by particle scattering and decay. One can also see that the relative difference between the average freeze-out coordinate and generation coordinate for quark coalescence is larger than that for particle scattering and decay.

Figure 2 shows the average transverse and longitudinal freeze-out coordinates (dashed lines) and generation coordinates (solid lines) of identical pions versus the particle transverse momentum in Pb-Pb collisions at $\sqrt{s_{NN}} =$ 2.76 TeV, where panel (a) is for all of the identical (negative) pions, (b) is for the pions generated by quark coalescence, and (c) is for the pions generated by particle scattering and hadron decays. In the calculations for Pb-Pb collisions, we take a pseudorapidity cut, $|\eta| < 0.8$, as in experimental data analyses [9]. One can see that the average coordinates are larger in Pb-Pb collisions at $\sqrt{s_{NN}} = 2.76$ TeV than in Au-Au collisions at $\sqrt{s_{NN}} = 200$ GeV.

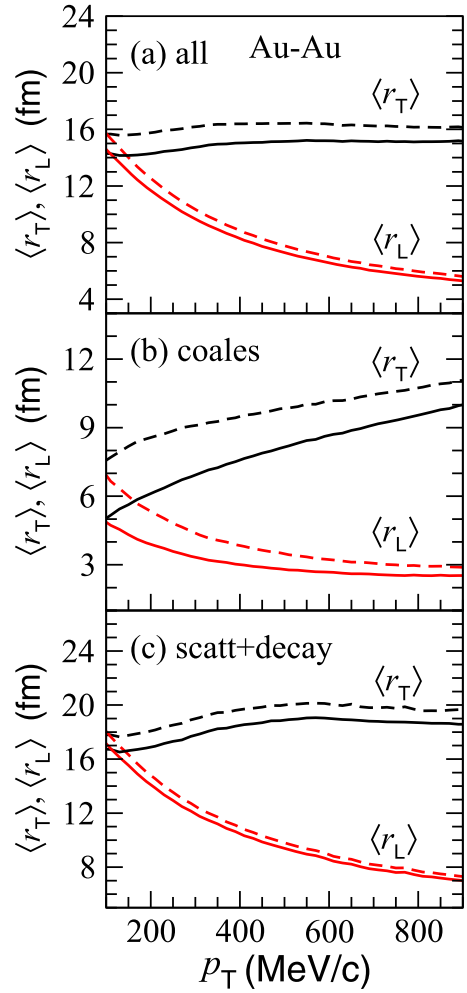

FIG. 1. Pion average transverse and longitudinal freeze-out coordinates (dashed lines) and generation coordinates (solid lines) in Au-Au collisions at $\sqrt{s_{NN}} = 200$ GeV. (a) All identical (negative) pions; (b) the pions generated by quark coalescence; and (c) the pions generated by particle scattering and decay.

III. TWO-PION HBT ANALYSES

A. Calculation of two-pion correlation function in AMPT model

The two-pion HBT correlation function is defined as

$$C(\mathbf{p}_1, \mathbf{p}_2) = \frac{P(\mathbf{p}_1, \mathbf{p}_2)}{P(\mathbf{p}_1)P(\mathbf{p}_2)}, \tag{1}$$

where $P(\mathbf{p}_i)\,(i = 1, 2)$ is the distribution of single-pion momentum $\mathbf{p}_i$, and $P(\mathbf{p}_1, \mathbf{p}_2)$ is the two identical pion momentum distributions in an event.

For a chaotic pion-emitting source, the denominator and numerator in Eq. (1) can be expressed, respectively,

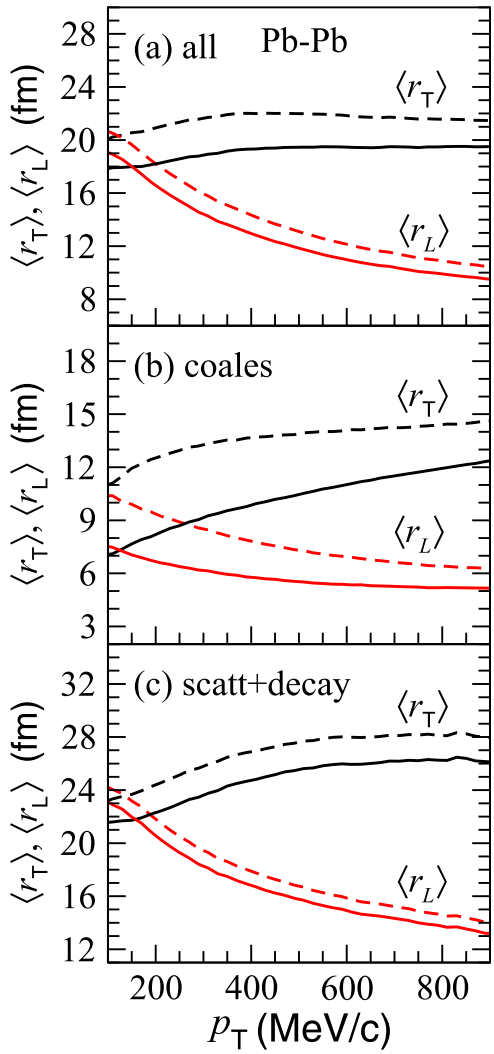

FIG. 2. Pion average transverse and longitudinal freeze-out coordinates (dashed lines) and generation coordinates (solid lines) in Pb-Pb collisions at $\sqrt{s_{NN}} = 2.76$ TeV. (a) All the identical (negative) pions; (b) the pions generated by quark coalescence; and (c) the pions generated by particle scattering and decay.

as [2]

$$P(\mathbf{p}_1)P(\mathbf{p}_2) = \sum_{X_1,X_2} A^2(\mathbf{p}_1, X_1)A^2(\mathbf{p}_2, X_2), \tag{2}$$

$$P(\mathbf{p}_1, \mathbf{p}_2) = \sum_{X_1,X_2} |\Phi(\mathbf{p}_1, \mathbf{p}_2; X_1, X_2)|^2, \tag{3}$$

where $A(\mathbf{p}_i, X_i)$ is the magnitude of the amplitude for emitting a pion with momentum $\mathbf{p}_i$ at four-coordinate X_i (freeze-out coordinates), and

$$\Phi(\mathbf{p}_1, \mathbf{p}_2; X_1, X_2) = \frac{1}{\sqrt{2}}\big[A(\mathbf{p}_1, X_1)A(\mathbf{p}_2, X_2)e^{ip_1\cdot X_1}e^{ip_2\cdot X_2} + A(\mathbf{p}_1, X_2)A(\mathbf{p}_2, X_1)e^{ip_1\cdot X_2}e^{ip_2\cdot X_1}\big], \tag{4}$$

where p_i is the four-momentum.

Because the HBT effect works on the identical pion pair with small relative momentum $\mathbf{q} = \mathbf{p}_1 - \mathbf{p}_2$, we can substitute $A(\mathbf{p}_j, X_i)$ for $A(\mathbf{K}, X_i)$ $(i, j = 1, 2)$ [smoothed approximation, $\mathbf{K} = (\mathbf{p}_1 + \mathbf{p}_2)/2$]. Then we have

$$\begin{aligned} P(\mathbf{p}_1, \mathbf{p}_2) &= \sum_{X_1,X_2} A^2(\mathbf{K}, X_1)A^2(\mathbf{K}, X_2)\{1 + \cos[(p_1 - p_2) \\ &\quad \cdot(X_1 - X_2)]\} \\ &= \sum_{X_1,X_2} A^2(\mathbf{p}_1, X_1)A^2(\mathbf{p}_2, X_2)\{1 + \cos[(p_1 - p_2) \\ &\quad \cdot(X_1 - X_2)]\}. \end{aligned} \tag{5}$$

In relativistic heavy-ion collisions at the RHIC and LHC, the systems are initially compressed in the beam direction (longitudinal or z direction) and then expand longitudinally and transversely. A partially coherent pion-emitting source was constructed in the AMPT model by introducing a coherent emission length L_C to the longitudinal freeze-out coordinates of identical pions [33]. It is assumed that the emissions of the two pions are coherent if they have a longitudinal distance of freeze-out coordinates less than L_C. However, a constant coherent emission length is too simple. Pions, as the lightest hadron, have wide de Broglie wavelengths, $(h/|\mathbf{p}|)$. Considering the systems produced in relativistic heavy-ion collisions are anisotropic in longitudinal and transverse directions, we respectively introduce longitudinal and transverse coherent emission lengths as

$$L_{CZ} = a_Z\left[\frac{h}{k_{1Z}} + \frac{h}{k_{2Z}}\right] \tag{6}$$

and

$$L_{CT} = a_T\left[\frac{h}{k_{1T}} + \frac{h}{k_{2T}}\right], \tag{7}$$

where a_Z and a_T are two coherent-length parameters determined by comparing model HBT results with experimental data, and k_{iZ} and k_{iT} $(i = 1, 2)$ are pion longitudinal and transverse generation momenta. We assume that the emissions of two pions with differences of longitudinal and transverse generation coordinates respectively smaller than L_{CZ} and L_{CT} are coherent. For this partially coherent source, we have

$$P(\mathbf{p}_1, \mathbf{p}_2) = \sum_{X_1,X_2} A^2(\mathbf{p}_1, X_1)A^2(\mathbf{p}_2, X_2)R(\mathbf{p}_1, \mathbf{p}_2; X_1, X_2), \tag{8}$$

where

$$R(\mathbf{p}_1, \mathbf{p}_2; X_1, X_2) = 1, \text{ for } \Delta z < L_{CZ} \text{ and } \Delta r_T < L_{CT}, \tag{9}$$

and

$$R(\mathbf{p}_1, \mathbf{p}_2; X_1, X_2) = 1 + \cos[(p_1 - p_2)\cdot(X_1 - X_2)], \quad \text{otherwise}, \tag{10}$$

where $\Delta z = |z_1 - z_2|$, $\Delta r_T = \sqrt{(x_1 - x_2)^2 + (y_1 - y_2)^2}$, and (x_i, y_i, z_i) $(i = 1, 2)$ are the pion generation coordinates.

Figures 3(a)–3(c) show the two-pion correlation functions $C(q)$ calculated with all of the identical (negative) pions, the pions generated by quark coalescence, and by particle scattering and decay, respectively, in Au-Au collisions at $\sqrt{s_{NN}} =$ 200 GeV and with impact parameter $0 < b < 3$ fm in the AMPT model. The correlation functions for the pions generated by quark coalescence are wider than those for the pions

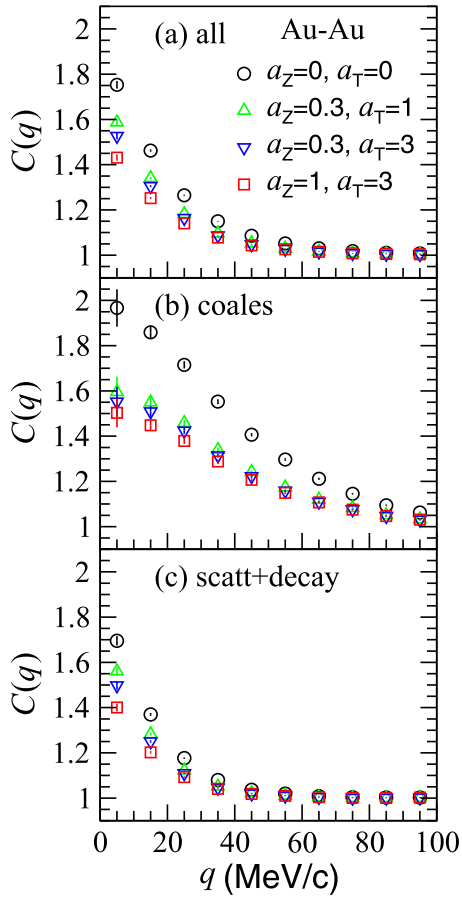

FIG. 3. Two-pion correlation functions $C(q)$ for pion-emitting sources with different coherent-length parameters, ($a_Z = 0$, $a_T = 0$), ($a_Z = 0.3$, $a_T = 1$), ($a_Z = 0.3$, $a_T = 3$), and ($a_Z = 1$, $a_T = 3$), in Au-Au collisions at $\sqrt{s_{NN}} = 200$ GeV, with impact parameter $0 < b < 3$ fm in the AMPT model. Results calculated with (a) all of the identical (negative) pions, (b) the pions generated by quark coalescence, and (c) the pions generated by particle scattering and decay.

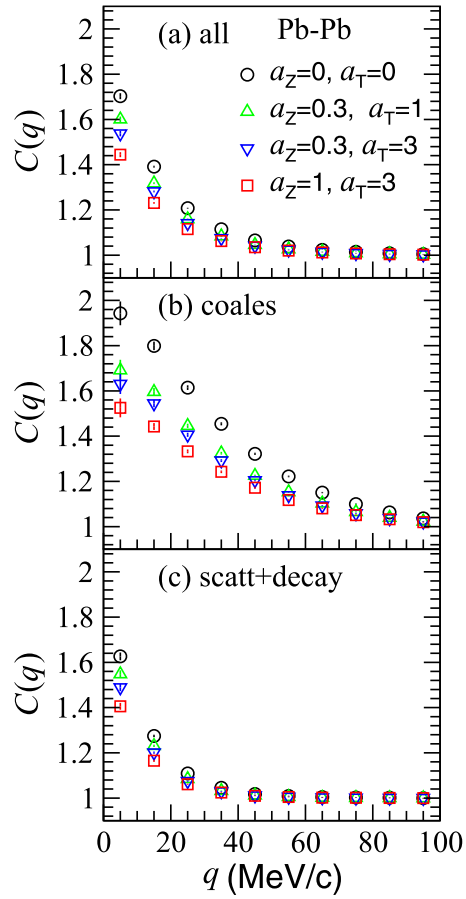

FIG. 4. Two-pion correlation functions $C(q)$ for pion-emitting sources with different coherent-length parameters, ($a_Z = 0$, $a_T = 0$), ($a_Z = 0.3$, $a_T = 1$), ($a_Z = 0.3$, $a_T = 3$), and ($a_Z = 1$, $a_T = 3$), in Pb-Pb collisions at $\sqrt{s_{NN}} = 2.76$ TeV, with impact parameter $0 < b < 3$ fm in the AMPT model. Results calculated with (a) all of the identical (negative) pions, (b) the pions generated by quark coalescence, and (c) the pions generated by particle scattering and decay.

generated by particle scattering and decay, because the former have smaller average freeze-out coordinates (see Fig. 1). In Figs. 3(a)–3(c), the circle, up-triangle, down-triangle, and square symbols denote the coherent-length parameters ($a_Z = 0$, $a_T = 0$), ($a_Z = 0.3$, $a_T = 1$), ($a_Z = 0.3$, $a_T = 3$), and ($a_Z = 1$, $a_T = 3$), respectively. One can see that the correlation function values for the partially coherent sources are less than those for completely chaotic sources ($a_Z = a_T = 0$) at small relative momenta. Also, one can see that the difference between the correlation functions of a partially coherent source and chaotic source at small q is greater for the quark coalescence generation than that for the generation of particle scattering and decay. This is because that the smaller average generation coordinates for quark coalescence generation lead to a greater effect than that for the generation of particle scattering and decay, with the same coherent-length parameters.

Figures 4(a)–4(c) respectively show the two-pion correlation functions $C(q)$ calculated with all of the identical (negative) pions, the pions generated by quark coalescence, and the pions generated by particle scattering and decay in Pb-Pb collisions at $\sqrt{s_{NN}} = 2.76$ TeV and with impact parameter $0 < b < 3$ fm in the AMPT model, where the circle, up-triangle, down-triangle, and square symbols mean the same as in Fig. 3. Compared to the correlation functions in Au-Au collisions, the two-pion correlation functions in Pb-Pb collisions are narrower because the average source sizes in Pb-Pb collisions are larger.

B. Interferometry results

In two-pion HBT analyses, the fitting correlation function is usually the Gaussian form,

$$C(q_{\rm out}, q_{\rm side}, q_{\rm long}) = \kappa\left(1 + \lambda\, e^{-q^2_{\rm out}R^2_{\rm out} - q^2_{\rm side}R^2_{\rm side} - q^2_{\rm long}R^2_{\rm long}}\right), \tag{11}$$

where $q_{\rm out}$, $q_{\rm side}$, and $q_{\rm long}$ are the Bertsch-Pratt variables [38,39], which respectively denote the components of the relative momentum $\mathbf{q}$ in the transverse "out" (parallel to the transverse momentum of the pion pair $\mathbf{K}_T$), transverse "side" (in the transverse plane and perpendicular to $\mathbf{K}_T$), and longitudinal ("long") directions in the longitudinally comoving

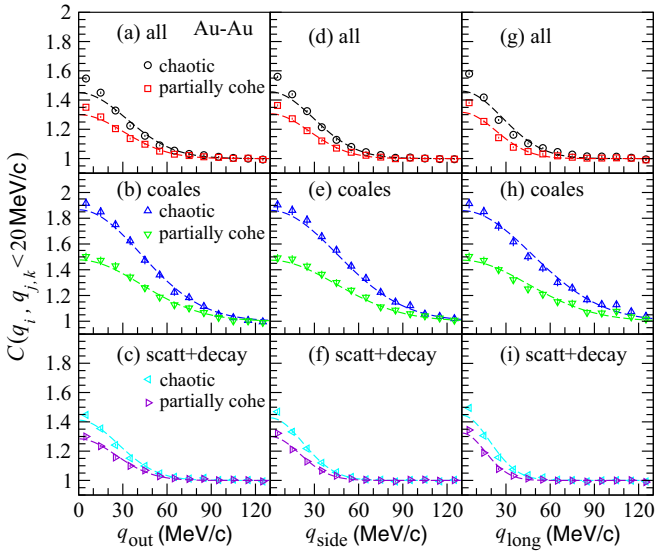

FIG. 5. Two-pion correlation functions with respect to relative momenta $q_{i,j,k}$ (i, j, k = out, side, long) for chaotic and partially coherent sources in Au-Au collisions at $\sqrt{s_{NN}} = 200$ GeV with impact parameter $0 < b < 3$ fm in the AMPT model. (Top) All of the pions, (middle) pions generated by quark coalescence, and (bottom) pions generated by particle scattering and decay.

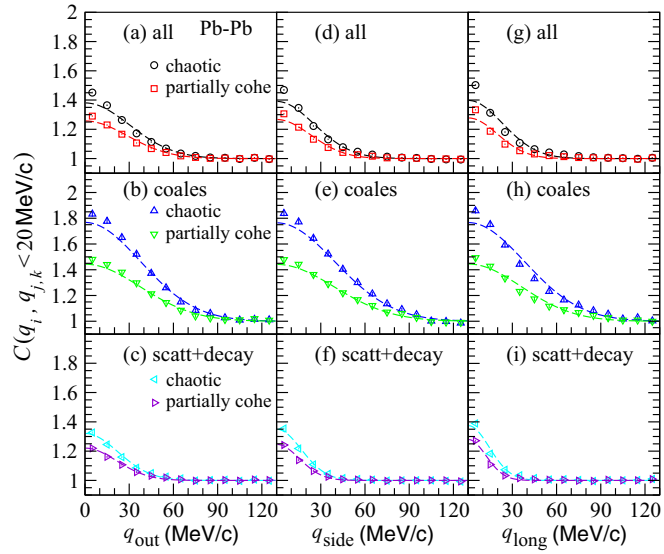

FIG. 6. Two-pion correlation functions with respect to relative momenta $q_{i,j,k}$ (i, j, k = out, side, long) for chaotic and partially coherent sources in Pb-Pb collisions at $\sqrt{s_{NN}} = 2.76$ TeV, with impact parameter $0 < b < 3$ fm in the AMPT model. (Top) All of the pions, (middle) pions generated by quark coalescence, and (bottom) pions generated by particle scattering and decay.

system (LCMS) frame [6]; κ is a normalization parameter; λ is the chaoticity parameter for the partially coherent source; and R_{out}, R_{side}, and R_{long} are the HBT radii in the respective out, side, and long directions.

Figure 5 shows projections of the two-pion correlation functions $C(q_{\mathrm{out}}, q_{\mathrm{side}}, q_{\mathrm{long}})$ in the out, side, and long directions for chaotic and partially coherent sources in Au-Au collisions at $\sqrt{s_{NN}} = 200$ GeV, with impact parameter $0 < b < 3$ fm in the AMPT model, where the top panels are for all of the identical pions, middle panels are for the pions generated by quark coalescence, and bottom panels are for the pions generated by particle scattering and decay. For each relative momentum direction, the projections of the correlation functions are obtained from the three-dimensional correlation functions by averaging the relative momenta in the other two directions over 0–20 MeV/c. Dashed lines in the figure are the fitting curves of Eq. (11). In the calculations the longitudinal and transverse coherent-length parameters for the partially coherent sources are taken as $a_{\mathrm{Z}} = 0.5$ and $a_{\mathrm{T}} = 1.8$, respectively, according to the comparison of the fitted HBT results in the AMPT model with experimental data [12] in different intervals of transverse momentum of the pion pair. The total number of events in the model calculations is 3×10^4.

Figure 6 shows projections of the two-pion correlation functions $C(q_{\mathrm{out}}, q_{\mathrm{side}}, q_{\mathrm{long}})$ in the out, side, and long directions for chaotic and partially coherent sources in Pb-Pb collisions at $\sqrt{s_{NN}} = 2.76$ TeV, with impact parameter $0 < b < 3$ fm in the AMPT model. In calculations in Pb-Pb collisions, the longitudinal and transverse coherent-length parameters for the partially coherent sources are taken to be $a_{\mathrm{Z}} = 0.8$ fm and $a_{\mathrm{T}} = 2.5$, respectively, according to the comparison of the fitted HBT results in the AMPT model with experimental data [9] in different intervals of transverse momentum of the pion pair. The total number of events in the mode calculations in Pb-Pb collisions is 6×10^3.

One can see that the intercepts of the correlation functions of partially coherent sources at zero relative momentum are lower than those of chaotic sources. This effect is most significant for the pions generated by quark coalescence and the least significant for the pions generated by particle scattering and decay. This is because the average generation coordinate of pions generated by quark coalescence is the smallest, and that of pions generated by particle scattering and decay is the largest.

Figure 7 shows the results of the fitted HBT radii R_{out}, R_{side}, and R_{long}, ratio $R_{\mathrm{out}}/R_{\mathrm{side}}$, and chaoticity parameter λ for chaotic and partially coherent sources in AMPT Au-Au collisions at $\sqrt{s_{NN}} = 200$ GeV, with impact parameter $0 < b < 3$ fm, in the transverse momentum intervals of pion pair $K_{\mathrm{T}} < 200$ MeV/c, $200 \leqslant K_{\mathrm{T}} < 300$ MeV/c, $300 \leqslant K_{\mathrm{T}} < 400$ MeV/c, $400 \leqslant K_{\mathrm{T}} < 500$ MeV/c, $500 \leqslant K_{\mathrm{T}} < 600$ MeV/c, and $600 \leqslant K_{\mathrm{T}} < 1000$ MeV/c. The experimental data in Au-Au collisions at $\sqrt{s_{NN}} = 200$ GeV with centralities 0%–5% and 10%–20% [12] are also shown in Figs. 7(a)–7(e) for comparison. We found that increasing the longitudinal coherent-length parameter a_{Z} leads to a decrease of λ and increase of R_{long}, while increasing the transverse coherent-length parameter a_{T} decreases λ and increases R_{side} and R_{out}. However, the increase of a_{T} does not improve the results of $R_{\mathrm{out}}/R_{\mathrm{side}}$. Finally, we took the longitudinal and transverse coherent-length parameters a_{Z} and a_{T} to be 0.5 and 1.8, respectively, for the partially coherent source. One can see that the model HBT radii and chaoticity parameter of the partially coherent source are closer to the experimental

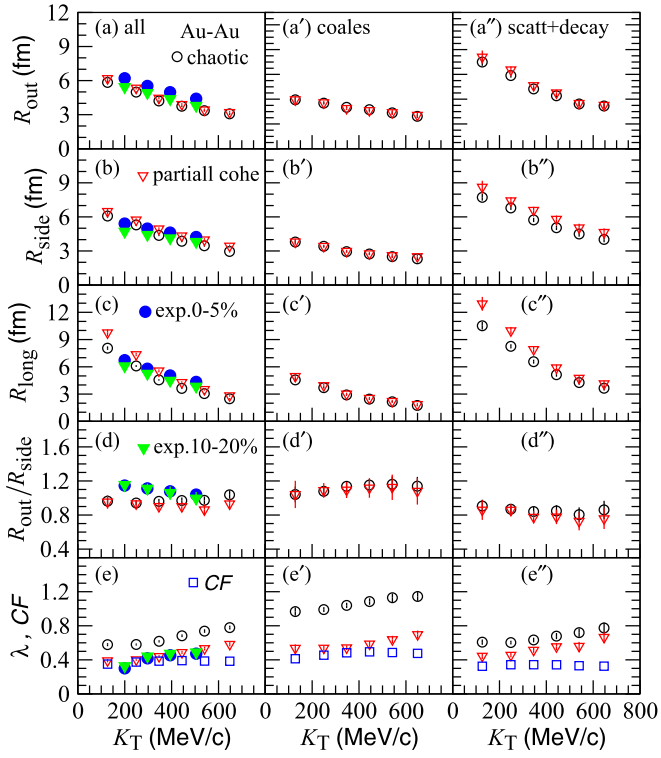

FIG. 7. Two-pion HBT results (R_{out}, R_{side}, R_{long}, R_{out}/R_{side}, λ) for the chaotic and partially coherent source and the coherent fraction (CF) of partially coherent source, with respect to transverse momentum of pion pair K_T, in Au-Au collisions at $\sqrt{s_{NN}} = 200$ GeV with impact parameter $0 < b < 3$ fm in the AMPT model. Experimental data [12] in Au-Au collisions at $\sqrt{s_{NN}} = 200$ GeV with centralities 0%–5% and 10%–20% are presented for comparison.

data compared to those of the chaotic source. The middle and right panels in Fig. 7 show the results for chaotic and partially coherent sources with the pions generated by quark coalescence and particle scattering and decay, respectively. One can see that the results of λ for quark coalescence show great differences between chaotic and partially coherent sources. However, the corresponding differences of λ values are small in the case of particle scattering and decay.

With the numbers of coherent-emission pion pairs $n_c = N_c(N_c-1)/2$ and total pion pairs $n_t = N_t(N_t-1)/2$, where N_c and N_t are the corresponding pion numbers, we can obtain the source coherent fraction $CF = N_c/N_t$. In Figs. 7(e), 7(e′), and 7(e″), the square symbols give the results of coherent fraction for the partially coherent source in Au-Au collisions at $\sqrt{s_{NN}} = 200$ GeV in the AMPT model. At small transverse momenta of the pion pair, the values of coherent fraction are mainly determined by pion longitudinal momentum. However, the decrease of coherent fraction with increasing K_T at large transverse momenta of a pion pair is mainly determined by the increase of pion transverse momentum at large transverse momenta of a pion pair, which leads to a decrease of L_{CT} [see Eq. (7)]. Table I presents the ratio of coherent pion-pair number to total pion-pair number, n_c/n_t, and the corresponding coherent fraction CF, where the superscripts (1), (2), and (3) are for the "all," "coales," and "scatt + decay" cases in Fig. 7, respectively. One can see that the results of $n_c^{(2)}/n_t^{(2)}$ are largest and the results of $n_c^{(3)}/n_t^{(3)}$ are smallest, because the average generation coordinate of the pions generated by quark coalescence is smallest and the average generation coordinate of the pions generated by particle scattering and decay is largest. This leads to the largest results of $CF^{(2)}$ and smallest results of $CF^{(3)}$. The result in the "(1)" case is between the results in the "(2)" and "(3)" cases.

Figure 8 shows the results of the fitted HBT radii R_{out}, R_{side}, and R_{long}, ratio R_{out}/R_{side}, and chaoticity parameter λ for chaotic and partially coherent sources in AMPT Pb-Pb collisions at $\sqrt{s_{NN}} = 2.76$ GeV, with impact parameter $0 < b < 3$ fm, in the transverse momentum intervals of pion pair $K_T < 250$ MeV/c, $250 \leqslant K_T < 350$ MeV/c, $350 \leqslant K_T < 450$ MeV/c, $450 \leqslant K_T < 550$ MeV/c, $550 \leqslant K_T < 650$ MeV/c, $650 \leqslant K_T < 750$ MeV/c, $750 \leqslant K_T < 850$ MeV/c, and $850 \leqslant K_T < 1200$ MeV/c. Figure 8 also shows the coherent fraction CF of partially coherent source in the AMPT model and the experimental data of HBT radii in Pb-Pb collisions at $\sqrt{s_{NN}} = 2.76$ GeV with centralities 0%–5% and 10%–20% [9] for comparison. The numerical results of CF are presented in Table II with the ratios n_c/n_t. The behaviors of the ratio n_c/n_t and coherent fraction CF in the cases for all the pions, the pions generated by quark coalescence, and the pions generated by particle scattering and decay are similar to those in Au-Au collisions.

In comprehensively comparing the model HBT radii R_{out}, R_{side}, and R_{long} with the experimental data, and the CF results with the values extracted from experimental measurements of multipion HBT correlations [7,14], we took the longitudinal and transverse coherent-length parameters a_Z and a_T to be

TABLE I. Ratio of coherent pion-pair number n_c/n_t and coherent fraction CF in Au-Au collisions at $\sqrt{s_{NN}} = 200$ GeV in the AMPT model. The superscripts (1), (2), and (3) are for all of the generated pions, the pions generated by quark coalescence, and the pions generated by particle scattering and decay, respectively.

Au-Au@200 GeV	$n_c^{(1)}/n_t^{(1)}$	$CF^{(1)}$	$n_c^{(2)}/n_t^{(2)}$	$CF^{(2)}$	$n_c^{(3)}/n_t^{(3)}$	$CF^{(3)}$
$K_T < 200$ MeV/c	0.122	0.350	0.170	0.413	0.106	0.325
$200 \leqslant K_T < 300$ MeV/c	0.140	0.374	0.207	0.455	0.117	0.343
$300 \leqslant K_T < 400$ MeV/c	0.148	0.385	0.233	0.483	0.118	0.343
$400 \leqslant K_T < 500$ MeV/c	0.153	0.391	0.244	0.494	0.117	0.342
$500 \leqslant K_T < 600$ MeV/c	0.149	0.386	0.236	0.486	0.110	0.331
$600 \leqslant K_T < 1000$ MeV/c	0.147	0.384	0.226	0.476	0.106	0.326

TABLE II. Ratio of coherent pion-pair number n_c/n_t and coherent fraction CF in Pb-Pb collisions at $\sqrt{s_{NN}} = 2.76$ TeV in the AMPT model. The superscripts (1), (2), and (3) are for all of the generated pions, the pions generated by quark coalescence, and the pions generated by particle scattering and decay, respectively.

Pb-Pb@2.76 TeV	$n_c^{(1)}/n_t^{(1)}$	$CF^{(1)}$	$n_c^{(2)}/n_t^{(2)}$	$CF^{(2)}$	$n_c^{(3)}/n_t^{(3)}$	$CF^{(3)}$
$K_T < 250$ MeV/c	0.100	0.316	0.133	0.364	0.086	0.293
$250 \leqslant K_T < 350$ MeV/c	0.106	0.326	0.146	0.382	0.089	0.298
$350 \leqslant K_T < 450$ MeV/c	0.103	0.321	0.145	0.381	0.082	0.287
$450 \leqslant K_T < 550$ MeV/c	0.099	0.314	0.140	0.374	0.077	0.277
$550 \leqslant K_T < 650$ MeV/c	0.093	0.305	0.130	0.360	0.072	0.268
$650 \leqslant K_T < 750$ MeV/c	0.088	0.297	0.121	0.347	0.068	0.260
$750 \leqslant K_T < 850$ MeV/c	0.083	0.289	0.111	0.334	0.064	0.252
$850 \leqslant K_T < 1200$ MeV/c	0.077	0.277	0.096	0.310	0.060	0.245

0.8 and 2.5, respectively, for the partially coherent source. One can see from Figs. 8(a)–8(e) that the model HBT radii of the partially coherent source are closer to the experimental data than those of the chaotic source. Also, the results of coherent fraction of the partially coherent source are consistent with the values 0.23 ± 0.08 extracted from the experimental measurement of three-pion HBT correlation functions [7] and $0.32 \pm 0.03(\text{stat}) \pm 0.09(\text{syst})$ extracted from the experimental measurement of four-pion HBT correlation functions [14]. The middle and right panels in Fig. 8 show the results for the chaotic and partially coherent sources with the pions generated by quark coalescence and particle scattering and decay, respectively. One can see that the differences between the λ values for chaotic and partially coherent sources are great in the case of quark coalescence. However, the differences of λ values between the chaotic and partially coherent sources are slight in the case of particle scattering and decay.

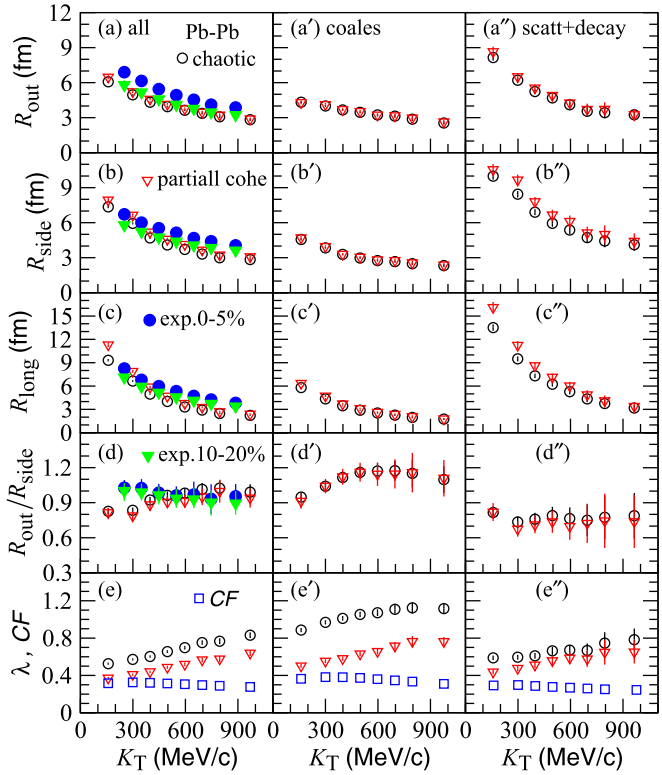

FIG. 8. Two-pion HBT results (R_{out}, R_{side}, R_{long}, R_{out}/R_{side}, λ) for the chaotic and partially coherent source and the coherent fraction (CF) of partially coherent source, with respect to transverse momentum of pion pair K_T, in Pb-Pb collisions at $\sqrt{s_{NN}} = 2.76$ TeV with impact parameter $0 < b < 3$ fm in the AMPT model. Experimental data [9] in Pb-Pb collisions at $\sqrt{s_{NN}} = 2.76$ TeV with centralities 0%–5% and 10%–20% are presented for comparison.

IV. SUMMARY AND DISCUSSION

We performed two-pion interferometry for pion-emitting sources in relativistic heavy-ion collisions in the AMPT model. A partially coherent source was constructed by introducing momentum-dependent longitudinal and transverse coherent emission lengths L_{CZ} and L_{CT}, based on pion de Broglie wavelength, in the calculations of two-pion HBT correlation functions. The two pions generated with longitudinal distance smaller than L_{CZ} and with transverse distance smaller than L_{CT} were assumed to be emitted coherently and without HBT correlation. We compared the HBT results in the AMPT model with experimental data in Au-Au collisions at $\sqrt{s_{NN}} = 200$ GeV and in Pb-Pb collisions at $\sqrt{s_{NN}} = 2.76$ TeV. We found that the HBT chaoticity parameter λ decreases with increasing L_{CZ} and L_{CT}. The results of HBT radii R_{out}, R_{side}, R_{long}, and chaoticity parameter λ of partially coherent sources in the AMPT model are closer to the experimental data in Au-Au collisions at $\sqrt{s_{NN}} = 200$ GeV at the RHIC compared to those of chaotic sources. Also, the results of R_{out}, R_{side}, and R_{long} of the partially coherent sources in the AMPT model are closer to the experimental data in Pb-Pb collisions at $\sqrt{s_{NN}} = 2.76$ TeV at the LHC compared to those of the chaotic sources. The results of a coherent fraction of partially coherent source in Pb-Pb collisions in the AMPT model are consistent with the values extracted by experimental measurements of multipion HBT correlations. We investigated the two-pion HBT results for chaotic and partially coherent sources constructed with the pions generated by quark coalescence and by particle scattering and decay, and found that the chaoticity parameter values of partially coherent sources are significantly less than those of chaotic sources for quark coalescence pions.

With the AMPT model, one can trace back a freeze-out particle to its generation coordinates, momentum, and parent. It is useful for studying the underlying physics of experimental

observables. The work presented in this paper provides a possible relationship between pion generation and the HBT observable, the two-pion correlation function. However, it does not affect the explanations that the AMPT model provides to other observables, such as single-particle spectra and collective flows. In this study the coherent-length parameters a_Z and a_T are determined by comparing the model HBT results with experimental data. They are model dependent. Physically, the parameters are related to the thermodynamical environment of particle production. Investigating the dependence of the coherent parameters on source thermodynamical properties and obtaining more general coherent parameters will be of interest. Pions, as the lightest hadron, may involve quantum effects in their production and propagation in the sources. It is possible that some of these effects remain and affect two- and multipion HBT correlations, the observables from quantum statistics. In relativistic heavy-ion collisions, the suppressions of two- and multipion HBT correlation functions at small relative momenta may indicate the pion-emitting sources are partially coherent. More detailed studies of the suppressions of pion HBT correlations in relativistic heavy-ion collisions will be of interest.

ACKNOWLEDGMENT

We thank Zi-Wei Lin for useful discussions and suggestions. This research was supported by the National Natural Science Foundation of China under Grant No. 12175031.

[1] M. Gyulassy, S. K. Kauffmann, and Lance W. Wilson, Phys. Rev. C **20**, 2267 (1979).
[2] C. Y. Wong, *Introduction to High-Energy Heavy-Ion Collisions* (World Scientific, Singapore, 1994), Chap. 17.
[3] U. A. Wienemann and U. Heinz, Phys. Rep. **319**, 145 (1999).
[4] R. M. Weiner, Phys. Rep. **327**, 249 (2000).
[5] T. Csörgő, Heavy Ion Phys. **15**, 1 (2002).
[6] M. A. Lisa, S. Pratt, R. Soltz, and U. Wiedemann, Annu. Rev. Nucl. Part. Sci. **55**, 357 (2005).
[7] B. Abelev (ALICE Collaboration) *et al.*, Phys. Rev. C **89**, 024911 (2014).
[8] J. Adam (ALICE Collaboration) *et al.*, Phys. Rev. C **92**, 054908 (2015).
[9] J. Adam (ALICE Collaboration) *et al.*, Phys. Rev. C **93**, 024905 (2016).
[10] C. Adler (STAR Collaboration) *et al.*, Phys. Rev. Lett. **87**, 082301 (2001).
[11] S. S. Adler (PHENIX Collaboration) *et al.*, Phys. Rev. Lett. **93**, 152302 (2004).
[12] J. Adams (STAR Collaboration) *et al.*, Phys. Rev. C **71**, 044906 (2005).
[13] B. I. Abelev (STAR Collaboration) *et al.*, Phys. Rev. C **81**, 024911 (2010).
[14] J. Adam (ALICE Collaboration) *et al.*, Phys. Rev. C **93**, 054908 (2016).
[15] Z. W. Lin and C. M. Ko, Phys. Rev. C **65**, 034904 (2002).
[16] Z. W. Lin and C. M. Ko, J. Phys. G **30**, S263 (2004).
[17] Z. W. Lin, C. M. Ko, B. A. Li, B. Zhang, and S. Pal, Phys. Rev. C **72**, 064901 (2005).
[18] M. Nasim, L. Kumar, P. K. Netrakanti, and B. Mohanty, Phys. Rev. C **82**, 054908 (2010).
[19] J. Xu and C. M. Ko, Phys. Rev. C **83**, 021903(R) (2011).
[20] D. Solanki, P. Sorensen, S. Basu, R. Raniwala, and T. K. Nayak, Phys. Lett. B **720**, 352 (2013).
[21] Y. L. Xie, G. Chen, J. L. Wang, Z. H. Liu, and M. J. Mang, Nucl. Phys. A **920**, 33 (2013).
[22] A. Bzdak and G. L. Ma, Phys. Rev. Lett. **113**, 252301 (2014).
[23] G. L. Ma and Z. W. Lin, Phys. Rev. C **93**, 054911 (2016).
[24] H. Li, L. He, Z. W. Lin, D. Molnar, F. Wang, and W. Xie, Phys. Rev. C **96**, 014901 (2017).
[25] M. R. Haque, M. Nasim, and B. Mohanty, J. Phys. G **46**, 085104 (2019).
[26] M. Dordevic, J. Milosevic, L. Nadderd, M. Stojanovic, F. Wang, and X. Zhu, Phys. Rev. C **101**, 014908 (2020).
[27] T. Shao, J. Chen, C. M. Ko, and Z. W. Lin, Phys. Rev. C **102**, 014906 (2020).
[28] K. J. Sun, C. M. Ko, and Z. W. Lin, Phys. Rev. C **103**, 064909 (2021).
[29] N. Magdy and R. A. Lacey, Phys. Rev. C **104**, 014907 (2021).
[30] S. Basu, V. Gonzalez, J. Pan, A. Knospe, A. Marin, C. Markert, and C. Pruneau, Phys. Rev. C **104**, 064902 (2021).
[31] N. Magdy, O. Evdokimov, and R. A. Lacey, J. Phys. G **48**, 025101 (2021).
[32] Z. Zhang, N. Yu, and H. Xu, Eur. Phys. J. A **58**, 240 (2022).
[33] G. Bary, W. N. Zhang, P. Ru, and J. Yang, Chin. Phys. C **45**, 024106 (2021).
[34] S. Y. Wang and W. N. Zhang, Front. Phys. **10**, 835592 (2022).
[35] X. N. Wang and M. Gyulassy, Phys. Rev. D **44**, 3501 (1991).
[36] B. Zhang, Comput. Phys. Commun. **109**, 193 (1998).
[37] B. A. Li and C. M. Ko, Phys. Rev. C **52**, 2037 (1995).
[38] G. Bertsch, M. Gong, and M. Tohyama, Phys. Rev. C **37**, 1896 (1988); G. Bertsch, Nucl. Phys. A **498**, 173c (1989).
[39] S. Pratt, T. Csörgő, and J. Zimányi, Phys. Rev. C **42**, 2646 (1990).